Migration study of organotin compounds from food packaging by surface-enhanced Raman scattering

Luisa Mandrile [a,*], Martina Vona [a, b], Andrea Mario Giovannozzi [a], Jesús Salafranca [c], Gianmario Martra [a, b], Andrea Mario Rossi [a]

[a] *Chemical Physics and Nanotechnology Department, National Institute of Metrological Research, Strada Delle Cacce 91, 10137, Turin, Italy*

[b] *Chemistry Department, University of Turin, Via Giuria 7, Turin, Italy*

[c] *Department of Analytical Chemistry, Aragon Institute of Engineering Research I3A, EINA-University of Zaragoza, Torres Quevedo Building, María de Luna 3, 50018, Zaragoza, Spain*

***** Corresponding author.

E-mail addresses: l.mandrile@inrim.it, luisamandrile89@gmail.com (L. Mandrile).

Abbreviations: Organotin compounds, (OTCs); Tributyltin, (TBT); Dibutyltin maleate, (DTM); Food contact materials, (FCM); Endocrine disrupting chemicals, (EDC); Tolerable daily intake, (TDI); Polyvinyl chloride, (PVC); Surface-enhanced Raman scattering, (SERS); Silver nanoparticles, (AgNPs); Acetic acid, (HAc); Calibration curve computing, (CCC); Weighted total least square, (WTLS); Montecarlo method, (MM).

Keywords: Organotin compounds; Surface-enhanced Raman scattering; Tributyltin; Dibutyltin maleate; Migration test; Food contact materials

ABSTRACT

The potential of surface-enhanced Raman scattering (SERS) has been investigated for the rapid analysis of two representative organotin compounds (OTCs): dibutyltin maleate (DTM) and tributyltin chloride (TBT), after migration tests from polyvinyl chloride (PVC), as a model food packaging material in aqueous food simulant (acetic acid 3% w/v). OTCs, often used as heat stabilizers additives for PVC, are classified as endocrine disrupting chemicals (EDCs) and their migration potential has to be controlled in compliance with the normative prescriptions for food contact materials. In this study, colloidal silver nanoparticles (AgNPs) were applied as liquid SERS substrate for direct-in-liquid analysis of food simulant after standardized migration tests of PVC samples spiked with OTCs. Promising results were obtained, reaching detection limits below the permitted limits for the considered OTCs (i.e. 0.15 mg/l): DTM and TBT were detected down to 0.01 mg/l and 0.08 mg/l, respectively. Calibration curves were calculated for standard solutions of DTM and TBT in the dynamic range between 0 and 1 mg/l (reduced $\chi^2 = 0.8$), and 0.5–5 mg/l (reduced $\chi^2 = 0.2$), respectively. Migrated TBT and DTM were detected in the food simulant, specifically identified and quantified by SERS, with a measurement uncertainty around 10% in all cases. In particular, it was found that TBT can migrate in higher amount compared to DTM when the PVC film is in contact with a slightly acidic matrix. These results were further confirmed by inductively coupled plasma-mass spectrometry and UV–Vis spectroscopy. In the present study, direct-in-liquid SERS approach showed to be very promising because it provides a fast response and it allows to overcome most of the common drawbacks of solid SERS substrates due to inhomogeneity problems and low repeatability.

1. Introduction

With the supermarket culture outbreak, consumers' habits have strongly changed and the development of new technologies to preserve food quality has become an outstanding need for food industries. Even though food packaging has been a remarkable breakthrough, recent studies on the potential interactions between food and containers have caused public concern [1]. Food contact materials (FCMs) are materials and articles intended for being in contact with food during its production, processing, storage, preparation and serving, before its possible consumption. FCMs include containers for transporting food, machinery to process food, packaging materials as well as kitchenware and tableware. FCMs should be sufficiently inert so that their constituents neither adversely affect consumer health nor influence the quality of food. FCMs are, indeed, an underestimated source of contaminants that can lead humans to be exposed to hazardous substances by food consuming [2]. To ensure the safety of FCMs and to facilitate the free movement of goods, the European Commission has drawn up a directive (Reg EC No 1935/2004, EC No 2023/2006) to regulate the production of FCMs and their placing on the market, ensuring high level of protection for consumers. A list of authorized substances, such as monomers, additives and polymer production aids, was subjected to restrictions and specifications as stated by the Commission Regulation (EC) No 10/2011 which tries to harmonize local laws of Member States on FCMs. In Art.11, it is defined that plastic constituents shall not be transferred into food in quantities exceeding a generic specific migration limit of 60 mg/kg. Moreover, in Art.12 it is specified that plastics shall not transfer their constituents in food simulants exceeding 10 mg of total components released per dm^2 of food contact surface (Reg EU 2016/1416, EFSA 2007).

Polyvinyl chloride (PVC) is a worldwide leading synthetic polymer due to its great versatility in applications thanks to its high polarity, which allows the incorporation of a wide range of useful additives. It is usually employed for both long-term uses, such as pipes for the transportation of potable water, and short-term uses as food packaging [3]. However, even though PVC as food packaging presents several advantages, such as preservation of organoleptic properties and its easy processing, its use has aroused public concern because of the migration risk of additives and vinyl chloride monomer [4,5]. Among other commonly used additives, organotin compounds (OTCs) are chemicals containing at least one bond between a tin and a carbon atom generally used as PVC heat stabilizers [6]. Mono and di-alkyl tin derivatives are generally preferred as stabilizers because of their lower toxicity compared with tri and tetra-alkyl tin derivatives, since these latter are more soluble in lipids and can interact with human neurological system compromising the immunological system [7]. OTCs have been classified as endocrine disrupting chemicals (EDCs) and their tolerable daily intake (TDI) was lowered at 0.1 μg/kg body weight by EFSA's evaluation 70. Several methods have already been proposed in literature for the analysis of OTCs, mainly in environmental samples [8,9], including atomic absorption spectroscopy (AAS) [10,11], molecular absorption spectroscopy [12] gas chromatography (GC) [13–15], high or ultra-performance liquid chromatography (HPLC or UPLC) [16], capillary electrophoresis [17,18], fluorescence [19,20], colorimetric methods [21] and inductively coupled plasma-mass spectrometry (ICP-MS) [22,23], also in combination with HPLC and UPLC [24]. The main disadvantages of these methods include time-consuming extraction and derivatization steps before sample analysis. Although ICP-MS reaches very low detection limits, the OTCs structures cannot be identified and the interference of inorganic tin species cannot be eliminated. Among the detection techniques, tandem mass spectrometry (MS/MS) offers a

number of advantages, such as more selective separation, elemental specificity, low detection limits and high sensitivity, but it remains very costly and time consuming [25]. On the other hand, spectroscopy represents an increasingly adopted technique for contamination analysis in the food analysis field as a rapid, simple and non-destructive technique. For instance, UV–Vis absorption spectroscopy allows very fast and simple quantification of absorbing species based on Lambert-Beer law. Moreover, Raman spectroscopy represents a promising candidate for the detection of most molecular species with high specificity and sensitivity, especially in the presence of surface-enhanced Raman scattering (SERS). SERS is a physical phenomenon provided by plasmonically active metal nano-objects, which provoke the intensification of Raman signals thanks to the combination of a chemical and an electromagnetic effect [26]. SERS coupled with solid phase extraction was recently tested for the detection of OTCs, proving satisfactory sensitivity and the possibility to identify selective signals for quantification [27]. The scope of this work is to investigate the potential of SERS performed directly in liquid matrix as an alternative technique for the rapid, sensitive and specific identification of OTCs in food simulant after migration tests from PVC samples. The same simulant samples after migration tests were also measured with other established analytical techniques to compare the results and performances of the different approaches.

PVC samples, intentionally spiked with OTCs, were subjected to migration tests and the resulting simulants were analysed by three techniques in parallel: i) SERS, using colloidal AgNPs as active substrate, as a promising innovative method, ii) ICP-MS, as an established technique for the quantification of migrated tin and iii) UV–Vis absorption spectroscopy, as a very rapid and simple technique but not suitable for selective and highly sensitive analysis. The migratory behaviour from PVC cling films of two widely used OTCs is studied: dibutyltin maleate (DTM) and tributyltin chloride (TBT), which are usually added at 0.1% w/w, as established by legislation. Considering that for OTCs the specific migration limit (SML) is 0.05 mg of tin per kg of food (Reg Eu 2016/ 1416, EFSA 2007), the corresponding legal limits for DTM and TBT are 0.15 mg/l and 0.14 mg/l, respectively.

2. Materials and method

2.1. Reagents and materials

Tributyltin chloride (TBT, CAS 1461-22-9, 99%), dibutyltin maleate (DTM, 78-04-6, 95%), acetic acid (64-19-7, 99%), nitric acid (7697-37-2, 65%), tetrahydrofuran (109-99-9, 99.9%) and methanol (67-56-1, 99.9%) were purchased from Sigma-Aldrich (Madrid, Spain). Silver nitrate (7761-88-8, 99.0%), Sodium borohydride (16940-66-2, 99%) and trisodium citrate dihydrate (6132-04-3, 99%) were obtained from Sigma-Aldrich (Milan, Italy). As food simulant acetic acid 3% w/v (HAc 3%) was prepared in ultra-pure water from a Wasserlab Ultramatic GR system (Barbatáin, Spain). A 75 mg/l stock solution of TBT and 10 mg/l of DTM in HAc 3% were prepared. Standard solutions including different concentrations (0.005 mg/l, 0.01 mg/l, 0.05 mg/l, 0.1 mg/l, 0.5 mg/l, 1 mg/l, 2 mg/l, 5 mg/l) of analytes were obtained by diluting stock solution in food simulant. An industrial food grade PVC cling film (10 mm thickness) was used for evaluating OTCs migration into a food simulant. Spiked PVC films were prepared by dissolving 2.5 g PVC film in 100 ml of THF in a flat-bottomed flask. Once a limpid solution was obtained, four glass vials were filled with approximately 14 g of PVC solution in THF. Meanwhile, stock solutions of TBT and DTM (10000 mg/l) in THF were prepared. For each compound, two PVC films with high and low concentration levels

(l.c., h.c.) of OTCs were produced. After adding TBT and DTM in two different concentrations each, the solutions were transferred to Petri dishes to let the solvent evaporate: after approximately 24 h the THF was completely evaporated and spiked PVC films were obtained. A PVC film spiked with both TBT and DTM together was also prepared by following the same procedure. The desired concentration of OTCs was supplied by a stock solution of 10 g/l of both TBT and DTM in THF. In Table 1 the final amount of OTCs and corresponding amount of Sn in the prepared PVC films are reported. Values are expressed as mg/g of PVC.

Table 1: *TBT and DTM at low (l.c.) and high (h.c.) concentration on tested PVC samples. The uncertainty associated to all values is 0.1 mg/g, due to the balance precision used for gravimetric measurements*.

Samples	mg OTCs/g (PVC)	mg Sn/g (PVC)
PVC + TBT l.c.	0.7	0.3
PVC + TBT h.c.	74.1	27.0
PVC + DTM l.c.	0.6	0.2
PVC + DTM h.c.	70.4	23.9
PVC + OTCs l.c. (DTM and TBT 50:50)	0.7	0.3
PVC + OTCs h.c. (DTM and TBT 50:50)	75.0	26.1

2.2. Migration tests

For each PVC film a portion of 5 cm^2 were cut and weighted in glass vials, then 8.33 ml of simulant were added, based on proportional relationship established by the norm (1 dm^3 of simulant per 6 dm^2 of packaging) (Reg EU 10/2011) [28]. Taking into account that the solubility of metallic cations increases at low pH values, 3% acetic acid (w/v), food simulant B, was considered the most unfavourable case. Since our preliminary results (unpublished) demonstrated that release of tin is relatively fast, migration testing for 10 days at 40 ºC, instead of 60 ºC, were selected as representative conditions for storage above 6 months at room temperature and below, including hot-filling, according to Commision Regulation (EU) 2016/1416 amending and correcting chapter 2, section 2.1.4, of Regulation (EU) No 10/2011. After ten days, plastic materials showed some changes in colour and integrity, they were taken out from the vials and the simulants were analysed by SERS, ICP-MS and UV–Vis.

2.3. AgNPs preparation

Silver nanoparticles suspension with nominal diameter of 30 nm are routinely synthesized according to a stepwise seeded-growth procedure proposed by Wan et al., 2013 and applied in spectroscopic analysis [29, 30]. All glassware used in the synthesis is soaked in aqua regia (HCl: HNO_3 3:1 v/v), rinsed thoroughly in water and dried with nitrogen prior to use. Briefly, 4 nm AgNPs are prepared by adding 20 ml of a 1% (w/v) citrate solution and 75 ml of water in a round bottom flask and the mixture is heated in an oil bath to 70 ºC for 15 min. After that, 1.7 ml of a 1% (w/v) $AgNO_3$ solution is introduced in the mixture, followed by the quick addition of 2 ml of a 0.1% (w/v) freshly prepared ice-cooled $NaBH_4$ solution. The reaction

solution is kept at 70 ºC under vigorous stirring for 1 h and cooled down to room temperature. Water is added to bring the volume of the dispersion to 100 ml. The resulting AgNPs are used as starter seeds. To obtain larger AgNPs, stepwise seeding growth is employed. For the synthesis of AgNPs of 30 nm, 2 ml of a 1% citrate solution is mixed with 75 ml of water and brought to boiling for 15 min. Then, 10 ml of starter seed solution is added while vigorous mechanical stirring, followed by the addition of 1.7 ml of a 1% $AgNO_3$ solution. Vigorously mechanical stirring is kept for 1 h at reflux conditions. Then, 2 ml of a 1% citrate solution are added to the reaction solution together with 1.7 ml of a 1% $AgNO_3$ solution. Reflux with vigorous stirring continues for 1 h. This operation was then repeated once. Finally, the reaction solution is cooled down to room temperature and water was added to bring the volume to 100 ml. For SERS application, the AgNPs 30 nm were washed by centrifugation for 30 min at 8000 rpm, then the supernatant was carefully removed and the nanoparticles were re-dispersed in ultra-pure water, maintaining the same final volume.

AgNPs are characterized by transmission electron microscopy (TEM). TEM images were taken with a Jeol 3010 microscope (LaB6 source) operated at 300 kV. For the observation, a droplet of AgNPs suspension was deposited on a standard Cu grid coated with a lacey carbon film, waiting until dryness.

2.4. UV–Vis absorption measurements

UV–Vis absorption spectra were collected by Hach Lange (Linate, Italy) spectrophotometer. OTCs solutions were analysed in a quartz cuvette with an optical path of 1 cm, in the spectral range 200–500 nm with a resolution of 1 nm. UV–Vis measurements concerning AgNPs used for SERS investigation were collected in the spectral range 300–900 nm. An equal volume of AgNPs 30 nm and OTCs solutions were mixed in Eppendorf tubes and vigorously shaken, then 50 µl of the mixed suspension were diluted in water before UV–Vis analysis (1:40 ratio). For DTM quantification by UV–vis standard solutions at 0.0 mg/l, 0.1 mg/l, 0.5 mg/l, 1.0 mg/l, 1.5 mg/l and 2.0 mg/l were prepared in food simulant and measured with the same experimental procedure, to build a calibration curve.

2.5. SERS measurements

SERS spectra were collected using a dispersive Raman microscope (Thermo Scientific DXR Raman) equipped with a 20x long working distance (LWD) objective, which focalizes the laser beam into the liquid sample. Sample solutions were mixed with an equal volume of AgNPs suspensions and the liquid mixture is transferred to a multi-wells plate, which is placed on the microscope motorized stage under the Raman microscope objective. The excitation laser is focalized by the LWD objective into the well, close to the liquid surface, for immediate inliquid SERS measurements. An excitation laser at 532 nm with a laser power of 10 mW and a 50 µm slit spectrograph aperture were used. The Raman backscattered signal is directed via the same microscope objective towards a full range grating providing spectral resolution of 5 cm^{-1} (the grating groove density is 1200) and then collected by a CCD. Raman and SERS spectra were collected in the spectral range 150–3400 cm^{-1} with the acquisition time of 1 s for 20 exposures.

2.6. ICP-MS measurements

Agilent 7500a Series ICP-MS (Palo Alto, CA, USA) with argon as carrier gas (1.20 l/min) was used for tin quantification. Peristaltic pump parameters regulating the sampling from vials to the plasma torch were: speed 0.3 rps, uptake time 30 s, stabilization time 30 s. Ultra-pure water and nitric acid 5% w/v were used for washing step before and after every

series of measurements. In order to evaluate the equipment efficiency, autotuning test was performed each time the torch was switched on. The procedure, consisting of sampling a specific solution that includes standard concentration of several metals, provides parameters of sensibility that should comply with specific values. Firstly, three compounds of autotuning solution are evaluated ($^{7}Li > 6400$, $^{89}Y > 16000$, $^{205}Tl > 9600$), then oxides formation ($^{140}Ce/^{156}CeO$) and double charges' presence ($^{70}Ce^{2+}/^{140}Ce^{+}$).

Mass spectrometer was set on 'full quant spectrum' mode to observe the mass spectrum of elements previously selected, with an acquisition time of 2 s and 10 repetitions. Five tin isotopes were evaluated for sample detection: ^{116}Sn, ^{117}Sn, ^{118}Sn, ^{119}Sn, ^{120}Sn. The two isotopes of gallium (^{69}Ga and ^{71}Ga) were used as internal standard because of its low mass interferences with other elements and mass value not so far from those of Sn (according to the relative isotopic abundance Table).

The linear dynamic range of the equipment is limited to element concentrations (0.0 mg/l, 0.01 mg/l, 0.05 mg/l, 0.1 mg/l, 0.4 mg/l, 0.8 mg/l and 1 mg/l), therefore more concentrated solutions should be diluted before the analysis. Moreover, it was established that the instrumental response could be influenced by the solution matrix, especially by the organic component. Indeed, only solutions with a maximum percentage of 10% of organic phase can be analysed with ICPMS without compromising plasma stability.

After migration tests, simulants were analysed without any sample pre-treatment, only a dilution step at 1:40 ratio was performed before the analysis of unknown samples obtained by the migration tests of PVC samples additivated with high concentration of TBT and DTM.

2.7. Data analysis and calculations

SERS spectra were analysed with Omnic 9 software (Thermo Fisher Scientific). Two points straight baseline in the local minima at the side of the peak of interest was set for peak intensity calculation. SERS spectra of TBT were normalized with respect to the peak at 240 cm^{-1} of AgNPs. Calibration curves were calculated using CCC software by weighted total least square (WTLS) method, to consider both uncertainties on the y and x axes [31]. The standard deviation (s) of 3 repeated measurements was used as y uncertainty while the standard uncertainty associated to the concentration as x uncertainty. The uncertainty associated with the concentration values was calculated by combining together, according to the law of propagation of uncertainty, the different sources of uncertainties due to the purity of TBT and DTM (≥99%), the weighting procedure (analytical balance precision 0.1 mg) and the volume measurement (all Class A glassware with tolerance 0.06 ml and micropipettes with 0.001 ml precision were used). The reduced $\chi^2 < 1$ was considered to evaluate the quality of the fit. Given a new measured intensity y, corresponding to an unknown sample concentration, an estimate for such measurand can be derived by the curve of analysis obtained by inverting the equation of the calibration curve. The uncertainty associated with the results was obtained by the propagation of the probability distributions characterizing the fit parameters (linear for DTM and polynomial for TBT) and y. A Monte Carlo simulation was performed according to international guidelines, in which parameter estimates were considered distributed according to a multivariate normal distribution with covariance matrix equal to that determined during the calibration process, and intensity y distributed as a normal distribution with standard deviation equal to the repeatability uncertainty associated with y [32].

Limits of detection (LOD) and quantification (LOQ) were calculated with the blank

determination method: LOD = C_{blank} + 3s_{blank} and LOQ C_{blank} + 10s_{blank} for all calibration curves [33], where C_{blank} is the mean concentration obtained by applying the linear fit as a quantification curve to the blank spectrum and 3s_{blank} is the standard deviation associated to three C_{blank} determinations. For TBT quantification with SERS, a slightly different approach was needed because an invariant instrumental response was obtained in the range 0–0.5 mg/l, preventing the quantification. Since the increasing trend of the intensity as a function of concentration does not start from zero in this case, the LOD was determined as the concentration that provides a S/N > 3 where S is the signal intensity at 615 cm^{-1} (identified as characteristic TBT peak) and N is the standard deviation of the noise of the blank spectrum in the same spectral region. For LOQ calculation the threshold concentration of 0.5 mg/l was considered as C_{blank}.

3. Results and discussion

3.1. SERS measurements of migrated OTCs in food simulant

The Raman fingerprints of pure DTM and TBT were collected and the most characteristic peaks were assigned to the relevant bonds and functional groups [34,35] (Fig. 1). For DTM, the main characteristic peak is related to Sn–O vibrational stretching mode at 601 cm^{-1}, which is highlighted in the spectrum "b" of Fig. 1. In the range between 1600 and 1700 cm^{-1}, signals of the cyclic structure are shown: C–C double bond stretching (1620 cm^{-1}) and peaks related to the group O–C–O–Sn (1675 cm^{-1}) are partially overlapped. Besides, Sn–C stretching mode falls closer to 500 cm^{-1} (symmetric and asymmetric stretching modes fall at 526 cm^{-1} and 628 cm^{-1}, respectively) and in the range 800–1050 cm^{-1} signals of complex carbon skeletal vibration, belonging to butyl groups, appear. For pure TBT, instead, Raman signals were mostly referred to the vibrational modes of C–H groups, since it is a quite simple molecule, with one atom of tin surrounded by three alkyl chains. The signals at 2800-3000 cm^{-1} are characteristic of symmetric and asymmetric stretching of methyl and methylene groups; the region 650-1500 cm^{-1} includes several bands, which are referred to typical vibrational modes of butyl chains. Here the most intense band is related to the stretching mode of C–C bond at 1154 cm^{-1} and the peaks at 844, 884 and 1048 cm^{-1} are attributed to complex carbon skeletal vibration [34]. Finally, the region at 200-650 cm^{-1} is associated with tin bonds. Two intense and well separated peaks at 507 and 595 cm^{-1} are related to the Sn–C symmetric and asymmetric stretching vibrations, and with the higher number of butyl groups the band at 500-510 cm^{-1} generally grows. Moreover, at 210 cm^{-1} there is the bending vibration of C–Sn–C group and at 410 cm^{-1} a butyl skeletal vibration is visible. These two are present in both TBT and DTM Raman spectra, while the two peaks at 320 and 390 cm^{-1} belong to Sn–Cl stretching and are characteristic TBT [36].

The pure spectra of TBT and DTM show some characteristic peaks of the two OTCs which allow the discrimination between these two analytes by Raman spectroscopy. Since TBT and DTM share Sn-butyl groups, lots of Raman signals are equivalent, but DTM also shows typical peaks at 1600-1700 cm^{-1} of the maleic acid derivative and the Sn–O stretching mode. Even though Sn–O signal is overlapped to Sn–C stretching mode, in TBT spectrum two peaks related to Sn–Cl can be identified.

Since DTM and TBT were not revealed in the Raman spectra of 10 mg/l solutions in HAc 3%, which do not differ from the Raman spectrum of the blank (HAc 3%) (the spectra are available in supplementary material Fig. 1S), SERS strategy is needed to increase the sensitivity of the technique and to allow the detection of such analytes in solution. In

particular, a colloidal suspension of 30 nm AgNPs was used as liquid SERS substrate for the detection of the analytes in the sub ppm range. Detailed information on the characterization of the synthetized AgNPs used in this study are present in supplementary material (Fig. 2S, Table 1S).

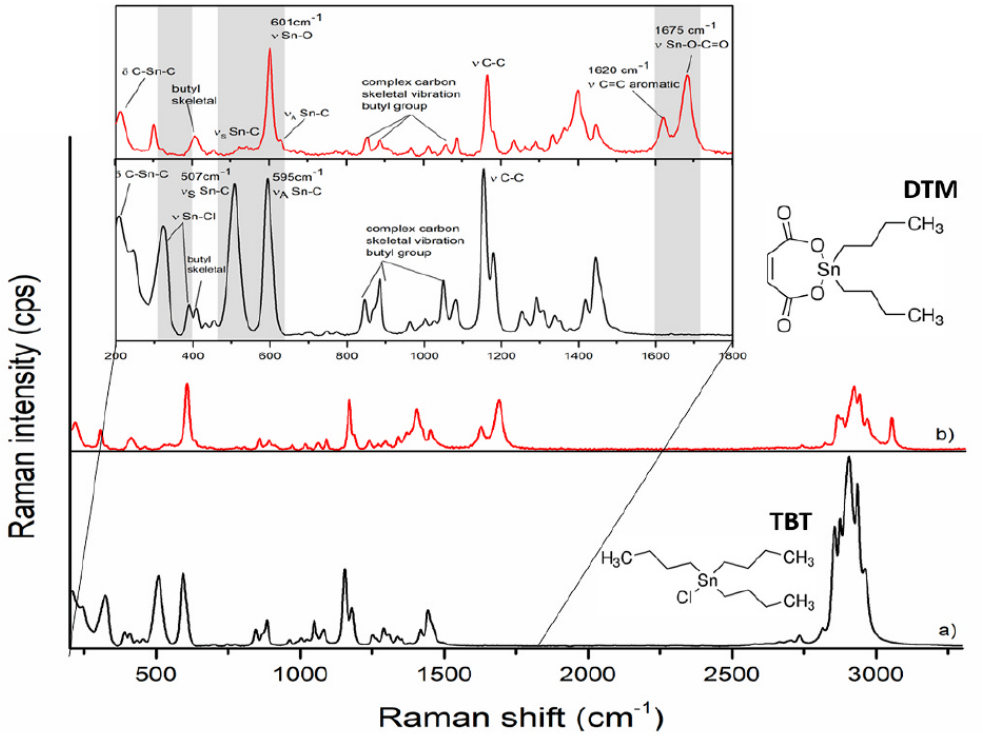

Fig. 1. Raman spectra of (a) pure tributyltin chloride (TBT) and (b) dibutyltin maleate (DTM) in solid state.

UV–Vis measurements were initially performed to evaluate the behaviour of the AgNPs in the food simulant solution (HAc 3%) and their interaction with OTCs, by monitoring the variation of the local surface plasmon resonance (LSPR) at 404 nm typical of the AgNPs, whose frequency is a function of particles size [37,38]. UV–Vis spectra give an indication of the agglomeration state of the AgNPs and, consequently, on the interaction of the matrix and the analytes with the SERS active substrate (Fig. 2). First, it was noticed that the AgNPs suspension turned from yellow to green when mixed with a solution of HAc 3% due to pH decrease from 4 to 3, which leads to the protonation of the carboxylic groups on the AgNPs surface and, consequently, to the formation of AgNPs clusters. Indeed, the UV–Vis spectrum of AgNPs mixed with HAc 3% shows a new absorption band at 636 nm due to AgNPs agglomerates. This means that the food simulant by itself is responsible for the agglomeration of AgNPs in suspension and SERS hotspots are formed in the liquid medium. However, further peculiar variations were registered in the UV–Vis spectra of the AgNPs in the presence of the analytes, indicating that the OTCs molecules can interact with the AgNPs, influencing the agglomeration process and probably remaining trapped in the hotspot regions, which are formed between two or more AgNPs upon agglomeration. In the presence of OTCs the 404 nm band associated with dispersed AgNPs decreases in intensity and a new band at 543 nm, and a second band at 698 nm in the case of DTM only, are formed. These new bands are associated with agglomerates and demonstrate that the agglomeration phenomenon that

occurs is, from one side assisted by the citrate protonations induced by the pH change, but also modulated by the presence of OTCs molecules.

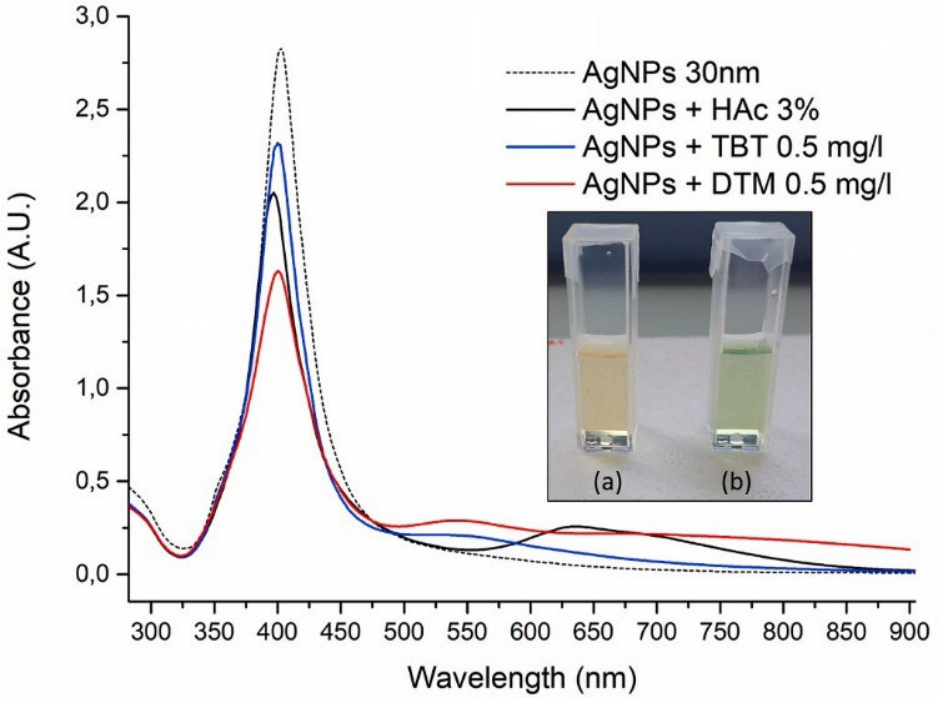

Fig. 2. UV–Vis spectra of native 30 nm AgNPs suspension in water (black dash), blank sample (AgNPs mixed with HAc 3%, black line) and AgNPs mixed with DTM (red line) and TBT (blue line) solutions at 0.5 mg/l in HAc 3%. In the inset figure the visual appearance of the native AgNPs colloids (a) and after agglomeration process (b). (For interpretation of the references to colour in this figure legend, the reader is referred to the Web version of this article.)

Thanks to the interaction between OTCs and the SERS substrate, specific SERS signals of these molecules appear in the SERS spectra of the suspensions. Indeed, even though an agglomeration is also stimulated in the blank sample and some signals were registered (AgNPs HAc 3% only, Fig. 3 spectrum a), specific peaks to be ascribed to TBT and DTM can be identified in the SERS spectra of the samples containing a certain concentration of them.

Comparing the normal Raman spectra of the pure DTM and TBT and their SERS counterparts in liquid medium at 5 mg/l, some spectral differences have emerged, as expected (Fig. 3 spectra b-e). Solubilized materials usually show spectral differences with respect to the corresponding crystalline powders, moreover SERS effect do not follow the same selection rules of normal Raman, therefore non-negligible variation between normal Raman and SERS fingerprints are usual. The SERS spectra of the two OTCs in HAc 3% can be distinguished in specific spectral ranges, marked with grey stripes in Fig. 3, where no interference from the blank is present. In particular, for DTM a large band between 500 and 650 cm^{-1} is present, due to the overlapping of Sn–O stretching (601 cm^{-1}) and Sn–C asymmetric stretching (595 cm^{-1}) modes (Fig. 3 spectrum b); whereas for TBT, only an intense and sharp peak at 610 cm^{-1} corresponding to Sn–C signal is present and two bands related to the complex skeletal vibration of butyl chains at 780 cm^{-1} (CH_2 rocking) and 880 cm^{-1} (CH_3 rocking) and Sn–Cl at 405 cm^{-1} are observed (Fig. 3 spectrum c). This latter, which was mentioned at 390 cm^{-1} in the normal Raman spectrum of pure TBT, is slightly shifted as a consequence of solubilisation

and most probably of the involvement of Cl atoms in the interaction mechanism with AgNPs. Also, the 3100 cm^{-1} band associated with aromatic CH vibration is only present for DTM, as well as the intense band between 1615 and 1725 cm^{-1} related to the complex vibration of the Sn–O–C–O group. However interfering signals are also present in this latter region in the blank, probably due to the AgNPs and their chemical environment. Therefore, it was not considered for the specific determination of OTCs by SERS. The spectral range in Fig. 3 is limited at 300 cm^{-1}, because at lower frequency (240 cm^{-1}) an intense band due to AgNPs clusters dominates the SERS spectra and no specific information of the two analytes can be obtained in that range.

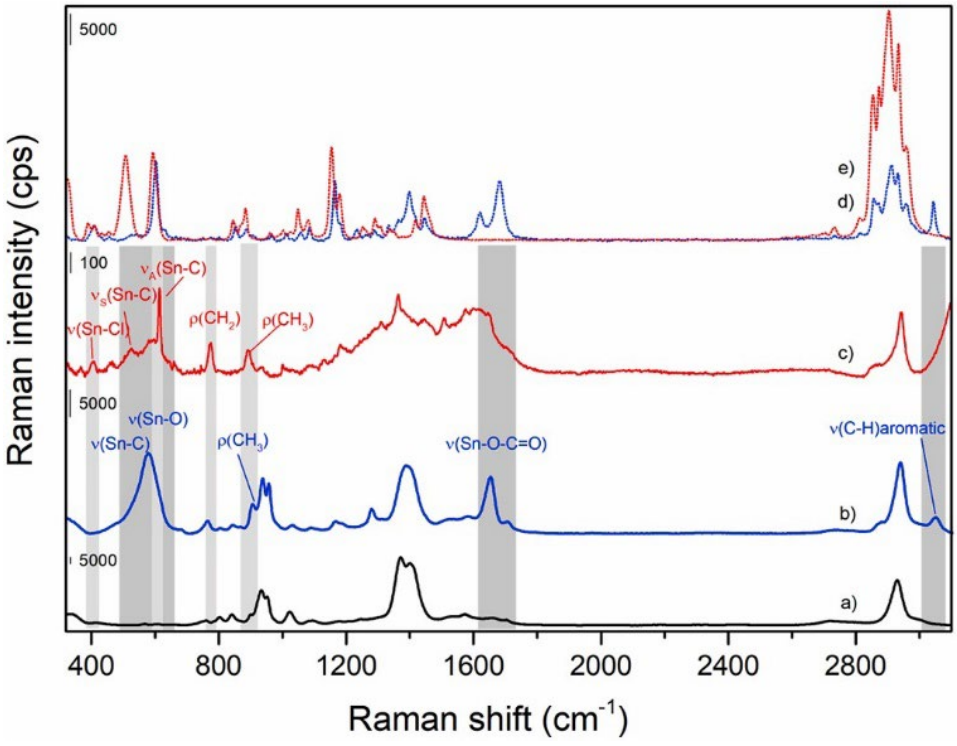

Fig. 3. SERS spectra of (a) the blank (AgNPs HAc 3%), (b) DTM 5 mg/l, (c) TBT 5 mg/l. Normal Raman spectra of pure DTM (d, blue dash) and TBT (e, red dash). (For interpretation of the references to colour in this figure legend, the reader is referred to the Web version of this article).

Standard solutions in a concentration range 0.00–1.00 mg/l of DTM in HAc 3% were tested (Fig. 4). As mentioned before, visible interaction occurred between AgNPs and the analyte and the suspensions' colour turned from green to dark green with a colour gradient compliant with the DTM concentration in solution. UV–Vis spectra, shown in Fig. 3Sa, revealed that higher concentration of DTM (5 mg/l) strongly induced agglomeration of nanoparticles. Indeed, the plasmonic peak intensity of single AgNPs at 400 nm was very low, but a broad band of agglomerates emerged between 550 and 700 nm. Spectra of DTM at 1.00, 0.50 and 0.01 mg/l presented a gradual decreasing intensity of plasmonic peak at 400 nm and an increasing intensity of the band at 548 nm as the DTM concentration increases. Finally, the shape of UV–Vis spectra corresponding to less concentrated solutions was similar to the blank spectrum (in black dash). This agglomerating effect caused by DTM is probably due to the presence of polar C–O groups able to establish hydrogen bonds with citrates, that surround the AgNPs surface, and induce a progressively more severe AgNPs agglomeration in the

suspension. The SERS spectra of DTM standard solutions showed a trend of the Raman intensity as a function of the analyte concentration. In particular, DTM distinctive Raman peaks at 595-610 cm^{-1} in SERS spectra shows a linear trend between 0 and 1 mg/l. For higher concentration a sort of saturation effect occurs and no further peak intensity increase is registered. This fact could also be due to the severe aggregation which impairs the AgNPs suspension stability, and consequently their SERS efficiency. For concentration levels higher than 0.1 mg/l the band is broad and not symmetric, located at 578 cm^{-1}; while at lower concentration the band splits into two peaks at 565 and 605 cm^{-1} (Fig. 4a). For the peak intensity evaluation the value of the local maximum between 550 and 580 cm^{-1} was considered for each spectrum. A calibration curve was obtained fitting the SERS intensity at 578 cm^{-1} peak and it shows a linear dynamic range between 0.01 and 1.0 mg/l (reduced χ^2 0.8) (Fig. 4b). The LOD and LOQ, calculated using the blank determination method, were 0.01 mg/l and 0.04 mg/l, respectively, which are lower than the low limits stated in the European Regulation (Reg CE 11/2011).

A similar approach was applied for SERS analysis of TBT. Standard solutions with progressively increasing concentration of TBT in HAc 3% were mixed with 30 nm AgNPs and a peculiar trend in sample colour was observed. AgNPs suspensions with low concentration of TBT appeared green, indicating a certain agglomeration of AgNPs in suspension; meanwhile the more concentrated solutions induced AgNPs to get an orange to yellow colour, as shown in Fig. 3Sc. The UV–Vis band of dispersed AgNPs at 404 nm increases as far as TBT concentration goes from 0.5 to 5 mg/l, contextually the band associated to agglomerates is gradually shifted from 650 to 548 nm and then disappeared (Fig. 3Sb). This dispersing effect caused by TBT could be explained by the mechanism of interaction of the TBT molecules with AgNPs, probably mediated by the Cl atom. It can be hypothesized that for low TBT concentration the agglomerative effect of HAc 3% on nanoparticles prevailed, whereas for high concentrations (starting from 0.5 mg/l) TBT seems to have a sort of dispersing ability and to provoke a visible change in the agglomeration state of the colloid.

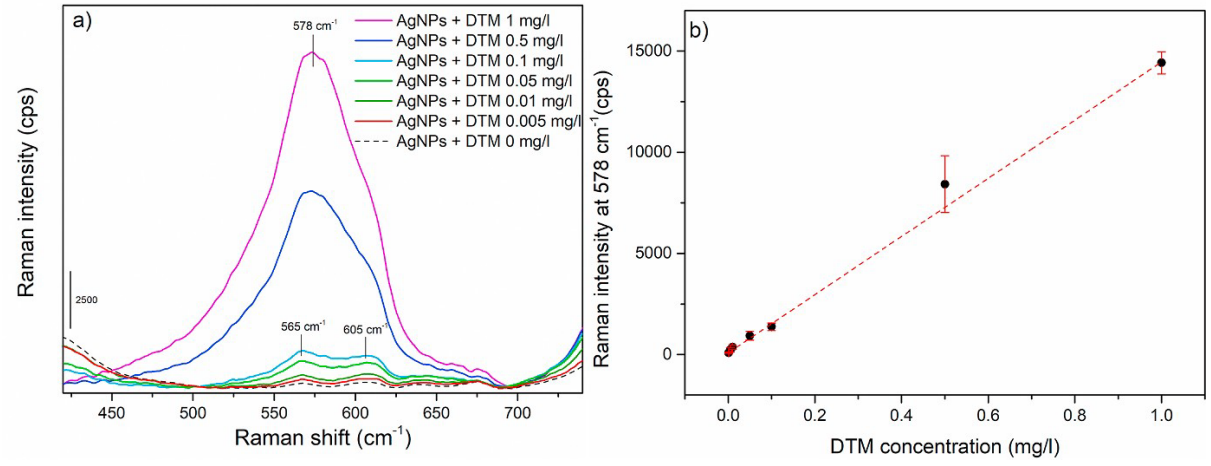

Fig. 4. SERS results of DTM analysis; a) SERS spectra of 30 nm AgNPs with DTM standard solutions in HAc 3% (from 0 to 1 mg/l); b) WTLS linear fit of SERS intensity at 550-580 cm^{-1}.

This interaction mechanism has strong consequences on the SERS response of the samples. Indeed, very intense SERS spectra were obtained for lower concentrations of TBT

(where SERS hotspots are present in the suspension thanks to the agglomeration state of AgNPs) and generally weaker signals were obtained as far as the concentration increases. Even though the SERS spectra of TBT concentrated solutions showed very low Raman intensity, some distinctive TBT peaks were observed, especially in the spectral range 500–660 cm^{-1}. SERS spectra were normalized with respect to the AgNPs peak at 240 cm^{-1} to overcome big intensity differences due to AgNPs agglomeration state and to compare TBT signals' intensity in the whole concentration range of interest (Fig. 4S). After normalization, the intensity of the TBT peak at 615 cm^{-1} increased proportionally with TBT concentration in the range 0.5–5 mg/l (Fig. 5a), and a second order polynomial calibration curve was calculated (reduced $\chi 2$ 0.2) (Fig. 5b). Conversely, an increase of peak intensity between 0.0 and 0.1 mg/l was not revealed, thus preventing the quantification in the range 0.0–0.5 mg/l. As previously noticed in UV–Vis spectra, the system undergoes a variation in the LSPR bands when TBT concentration reaches 0.5 mg/l, consequently a specific SERS signal of the TBT was registered from this concentration on, probably due to the TBT bonding on AgNPs surface. The obtained LOD and LOQ values for TBT calibration curve (considering 0.5 mg/l as offset concentration), were 0.10 mg/l and 1.53 mg/l, respectively.

The enhancement factor (EF) for both TBT and DTM was also calculated, following the procedure described in Ref. [39], and the resulting EF comes to 16 and $5.2x10^4$ for TBT and DTM, respectively. Details about the EF calculation and the procedure are reported in the supplementary information. The huge difference of several orders of magnitude in the EF value between TBT and DTM are mainly related to the different interaction mechanism and the agglomeration effect that such molecules induce in the AgNPs suspension, as previously described in the UV–Vis measurements. Since DTM induces a strong agglomeration of the AgNPs in respect to TBT, this leads to a huge enhancement of the Raman signal, which results in a higher sensitivity in DTM detection.

Once a SERS calibration curve was calculated for both analytes, unknown samples obtained from the migration test of PVC spiked with TBT and DTM, using HAc 3% as food simulant, were analysed by SERS. Seven samples were investigated: PVC blank, PVC spiked with a high and low concentration (h.c. and l.c., respectively, the corresponding concentration values are reported in Table 1) of DTM, PVC spiked with h.c. and l.c. of TBT, and PVC spiked with h.c. and l.c. of both OTCs. For DTM quantification in the simulant after migration tests, all spiked samples showed SERS signals that can be assigned to DTM. In Fig. 6a SERS spectra of PVC samples in the spectral range 500–700 cm^{-1} are reported, showing the vibrational band involving Sn bond used for the quantification. The peak intensity is meaningful for migration tests from PVC contaminated with high concentration levels, while in the other cases results below the LOQ were obtained, even though a detectable signal higher than LOD was registered. The simulant corresponding to PVC spiked with h.c. of DTM was quantified at 0.41 0.04 mg/l by using the calibration curve previously calculated.

Also simulants containing the migrated TBT from PVC films were analysed with SERS (Fig. 6b). However, in order to preliminary evaluate the concentration range of the unknown samples, UV–Vis analysis was first carried out (Fig. 5S). Mixing AgNPs with the simulants corresponding to PVC with TBT l.c., the suspensions turned to green and the UV–Vis spectra were comparable with the standards with low concentrations of TBT (not quantifiable range); samples with a higher concentration of TBT, instead, showed a yellow colour after mixing with AgNPs and their UV–Vis spectra followed the same trend of the more concentrated standard solutions. Since SERS quantification cannot be performed at lower concentrations,

only the samples with higher concentration of TBT were quantified. The simulant solution was quantified using the calibration curve previously calculated and a TBT concentration of 10.72 1.11 mg/l was detected, whereas l.c. samples provided results below the LOQ. Moreover, simulant solutions from PVC samples spiked with both analytes were analysed by SERS (Fig. 6c). In the spectral range between 500 and 700 cm^{-1}, two peaks respectively related to DTM and TBT characteristic vibrational bands were identified. Therefore, DTM and TBT migrated from PVC spiked with h.c. of OTCs were individually quantified in simulant by using calibration curves previously calculated, meanwhile low concentration samples showed results below the LOQ. DTM concentration detected was 0.12 ± 0.01 mg/l, whereas TBT concentration was 4.16 ± 0.11 mg/l.

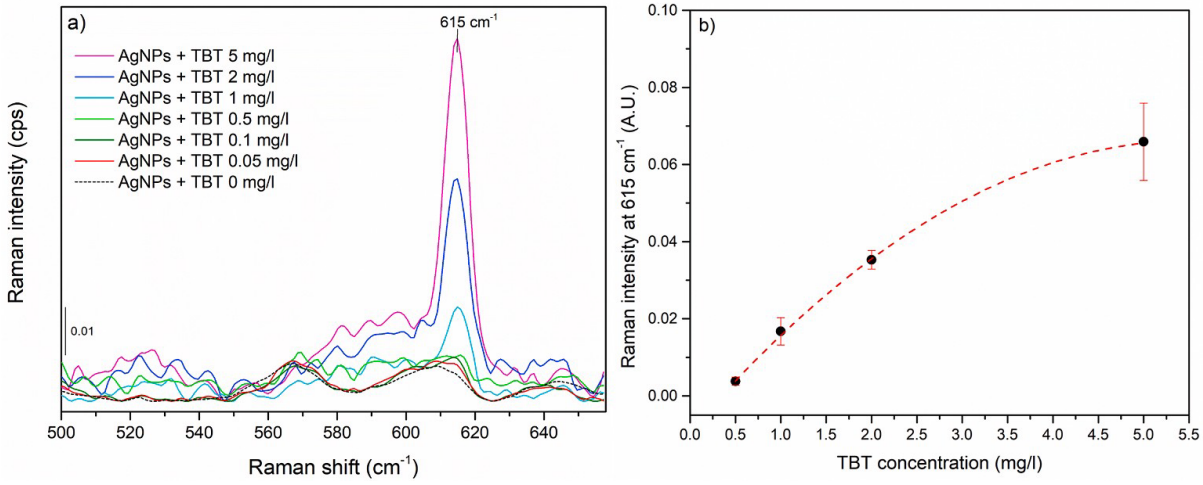

Fig. 5. SERS results of TBT analysis; a) normalized SERS spectra of 30 nm AgNPs with TBT in HAc 3% (from 0 to 5.0 mg/l); b) WTLS second order polynomial fit of SERS intensity at 615 cm^{-1}.

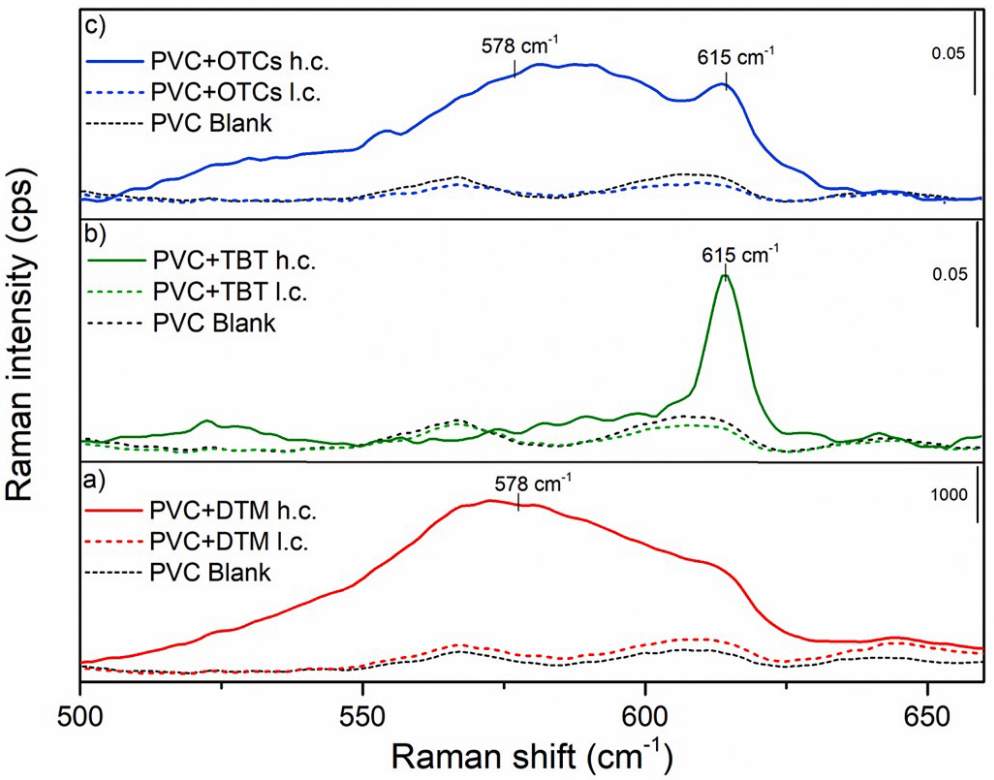

Fig. 6. a) SERS spectra of 30 nm AgNPs DTM migrated in HAc 3% from PVC samples; b) SERS spectra of 30 nm AgNPs TBT migrated in HAc 3% from PVC samples; c) SERS spectra of 30 nm AgNPs OTCs (both DTM and TBT) migrated in HAc 3% from PVC samples.

3.2. ICP-MS quantification of OTCs in food simulant after migration tests

Since EU directives expressed the presence of OTCs in food simulants as mg/kg of tin in the simulant, ICP-MS was applied for the quantification of tin in HAc 3% after migration tests from PVC samples.

Standard solutions were first analysed using ICP-MS in order to create appropriate calibration curves in the linear range between 1 µg/l and 1 mg/l. In Fig. 6Sa the calibration curve obtained for DTM in HAc 3% is reported (R2 0.99; LOD 0.005 mg/l; LOQ 0.007 mg/l), as well as for TBT in HAc 3% (R^2 = 0.99; LOD = 0.027 mg/l; LOQ = 0.092 mg/l).

After the migration tests, the amount of DTM and TBT migrated from PVC samples into the simulant was determined by ICP-MS and reported in Table 2, together with the quantitative results provided by the different techniques used in this study. PVC samples spiked with both OTCs could not be quantified using the calibration curves obtained by detecting one single additive because the technique cannot discern whether the Sn signal comes from DTM or TBT. Moreover, unusual matrix effects were noticed in presence of organic derivatives and a generic calibration curve built by using inorganic Sn standards did not lead to meaningful results. Simulant solutions of samples that did not fit the linearity range were diluted in HAc 3% and then a dilution factor (1:40) was considered in data processing.

503 **Table 2:** Data results of mg(Sn)/kg (simulant), analysed by using all the techniques reported.

	ICP-MS (mg/kg)	SERS (mg/kg)	UV–Vis (mg/kg)
PVC + DTM l.c	0.004 ± 0.001	> LOD; < LOQ	> LOD; < LOQ
PVC + TBT l.c	0.049 ± 0.021	> LOD; < LOQ	–
PVC + OTCs l.c.	–		> LOD; < LOQ
PVC + DTM h.c	0.273 ± 0.054	0.14 ± 0.02	0.14 ± 0.09
PVC + TBT h.c.	5.70 ± 2.52	3,91 ± 0.78	–
PVC + OTCs h.c.	–	DTM 0.04 ± 0.01 TBT 1.52 ± 0.04	DTM 0.21 ± 0.14 TBT –

504

505 ***3.3. UV–Vis quantification of DTM in food simulant after migration tests***

506 Since DTM derives from maleic acid and presents a cyclic structure with two carbonyl
507 groups and a C–C double bond, it shows an absorption band at 233 nm in the UV range and
508 the absorbance intensity of peaks presents a proportional trend according to DTM
509 concentration. Even though the sensitivity and specificity of UV–Vis determination are lower
510 than SERS, this technique was exploited to obtain an alternative quantification method to
511 confirm SERS results in a very rapid and simple way.

512 A calibration curve was obtained and reported in Fig. 7S. A linear dynamic range was
513 obtained between 0.1 and 2.0 mg/l (reduced $\chi^2 = 1.4$) and the LOD and LOQ were 0.08 mg/l
514 and 0.13 mg/l, respectively. The amount of DTM migrated in simulant HAc 3% from PVC
515 samples spiked with h.c. determined by UV–Vis was 0.40 ± 0.27 mg/l, while for l.c. samples
516 detectable signal higher than LOD was registered, but lower than the LOQ. UV–Vis
517 absorption peak was also detected in the simulants in contact with PVC additivated with both
518 OTCs, providing detectable but not quantifiable signal for l.c. level, and 0.61 ± 0.41 mg/l for
519 h.c. level (all quantitative results are collected in Table 3S for an easier comparison).
520 Unfortunately TBT does not present an evident characteristic absorption band in the UV–Vis
521 range, and a proper comparison was not possible for this analyte.

522 ***3.4. Comparison of results of the three techniques***

523 All the quantitative results on the OTCs migration from the different PVC samples
524 provided by ICP-MS, SERS and UV–Vis measurements are summarized in Table 2. Since the
525 European directive (Reg Eu 2016/ 1416, EFSA 2007) expresses the migration limit of OTCs
526 in food simulants as the amount of Sn (mg/kg), the concentration of OTCs was converted in
527 concentration of Sn, considering that each molecule of TBT and DTM includes one tin atom.

528 ICP-MS spectrometry was here employed as the most sensitive and traditional analytical
529 technique, without using any sample pretreatment or chromatographic separation as with
530 SERS and UV–Vis analysis, in order to directly quantify the amount of Sn in the samples. As
531 expected, ICP-MS was able to detect and quantify the Sn amount related to TBT and DTM in
532 the samples at both l.c. and h.c., demonstrating lower detection and quantification limits with
533 respect to SERS and UV–Vis. In fact, the presence of DTM and TBT in the less concentrated
534 PVC samples was in most cases detected by SERS and UV–Vis but at a concentration lower
535 than LOQ. As far as the quantification of the OTCs in the h.c samples is concerned, a

quantification of both TBT and DTM was provided by SERS, while UV–Vis was only able to quantify the DTM amount, as previously explained in the paragraph 3.3. Indeed, a complete comparison of the results among the different techniques can be only performed on the PVC TBT/DTM h.c. samples. A good agreement on the quantification of Sn migration was obtained by the comparison of SERS and UV–Vis on the PVC DTM h.c. sample, while ICP-MS registered a higher migration of DTM in this sample. A good agreement of the results provided by ICP-MS and SERS was also obtained for the quantification of the TBT in the PVC + TBT h.c. In particular, when considering the analytical performances of the ICP-MS, a high relative measurement uncertainty was observed for almost all the analysed samples, ranging from 20% to 50% in some cases. This was mainly related to the organic matrix effect that interfered with Sn detection, which potentially affected the accuracy of the measurement and also led to meaningless results in Sn quantification, when both OTCs are present. In the latter case, the quantification of Sn by ICP-MS was not possible, as previously explained in paragraph 3.2, whereas, in this study, SERS was the only technique able to contemporarily detect both analytes, because the quantification is based on distinctive signals for each compound. However, since a competing mechanism occurs between TBT and DTM in the interaction with the AgNPs, this probably leads to an underestimation of the DTM quantification by SERS in the PVC + OTCs h.c. sample, as shown by the comparison with UV–Vis results. The reliability of the UV–Vis is corroborated by the coherent DTM migration from PVC DTM h.c. and PVC OTCs h.c. expressed as migrated Sn% of 0.4% and 0.3% respectively (see Table 2S). To better understand the origin of discrepancies sometimes occurring between the quantitative results, further investigations would be required to refine the ICP-MS methodology and to set a new standard procedure to evaluate and compare the accuracy of all the techniques. However, even though the quantification results were not always in good agreement, the amount of TBT and DTM migrated from the PVC films was in the same order of magnitude for all the employed techniques and this can give at least an indication of the migratory capability of these compounds in food simulant. In particular, TBT migration was higher compared to DTM, probably because no bulky groups are present. Moreover, if we consider that the EU SMLs for organotin compounds is 0.05 mg Sn/kg simulant, the present results demonstrate that in most of the considered cases the European limit was exceeded, except for PVC spiked with low concentration of DTM. Such a result is more evident if the overall migration of tin from the samples is evaluated by considering the initial amount of tin added in PVC films and the migrated Sn. In Table 2S, the percentage of migrated tin is reported for each PVC sample, providing that in general TBT tends to migrate more than DTM.

4. Conclusions

SERS was used to detect two representative compounds belonging to the class of OTCs, often used as additives in plastic materials, also for food packaging. We tested the migratory behaviour of DTM and TBT from PVC films into a common food simulant suggested by the normative in vigour (HAc 3%, representative for slightly acidic foods). AgNPs colloids were used as SERS substrate for measurements directly in liquid medium. Promising results were obtained in terms of detection and quantification limits of the technique, reaching LOD well below the concentration limits stated by the norms in vigour for OTCs. In particular DTM was detected down to 0.01 mg/l and TBT down to 0.1 mg/l in food simulant solutions. Moreover proportionality between the intensity of characteristic Raman peaks of OTCs and

their concentration was demonstrated in the concentration range of interest for application purposes. Standard solutions of DTM and TBT in HAc 3% were analysed for preparing calibration curves. The dynamic range for DTM was 0–1 mg/l (reduced $\chi^2 = 0.8$), and for TBT 0.5–5 mg/l (reduced $\chi^2 = 0.2$). This is a particularly interesting result since very often univariate calibration of SERS intensity against the analyte concentration is not achieved, due to the non-proportional behaviour of the enhancement effect as a function of concentration. As it is known, the dynamic range, suitable for quantification, in SERS measurements is usually narrow or completely absent because of homogeneity problems of SERS substrates, low repeatability. However, in this paper we showed that in liquid approach can be successfully applied to overcome most of these drawbacks. Migrated TBT and DTM in the simulant were detected, specifically identified and quantified by SERS measurements, with a measurement uncertainty lower than 20% in all cases. Even though the molecular structures of TBT and DTM have chemical groups in common and show similarities in their Raman spectra, it is possible to observe peaks that are specific for TBT and DTM, providing selective additive identification. Moreover, it was found out that TBT can migrate in greater amount compared to DTM when the PVC film is in contact with a slightly acidic matrix.

In the light of the discussed results, SERS represents a promising technique for screening analysis (detection and identification of molecular additives). It allows rapid tests with versatility, high sensitivity and specificity, with limited sample preparation procedures and less solvent wasting than other techniques.

Authors contribution

L.M., A.G., J.S., M.V. Conceptualization; M.V., L.M. Data curation; M.V., L.M. Formal analysis; J.S., G.M., A.R. Funding acquisition; M.V., L. M., A.G., Investigation; L.M., A.G., J.S. Methodology; A.R., J.S., G.M. Project administration; A.R., J.S. Resources; A.R., J.S. Software; A.R., J. S., G.M. Supervision; A.G., A.R., J.S., G.M. Validation; All Visualization; L.M., M.V. Writing-original draft; All authors Writing-review & editing

Declaration of competing interest

The authors declare that they have no known competing financial interests or personal relationships that could have appeared to influence the work reported in this paper.

Acknowledgments

The authors want to acknowledge Dr. Iris Cagnasso and Matteo Berruto for silver nanoparticles preparation and technical assistance, and Dr. Cristina Nerín for the Analytical Chemistry laboratory facilities at the University of Zaragoza. This research was in part performed in the IMPreSA Infrastructure laboratories, funded by Regione Piemonte and INRIM. This research did not receive any specific grant from funding agencies in the public, commercial, or not-for-profit sectors.

Appendix A. Supplementary data

Supplementary data to this article can be found online at https://doi.org/10.1016/j.talanta.2020.121408.

References

[1] J.H. Hotchkiss, Food-packaging interactions influencing quality and safety, Food Addit.

Contam. 14 (1997) 601–607.

[2] J. Muncke, Endocrine disrupting chemicals and other substances of concern in food contact materials: an updated review of exposure, effect and risk assessment, J. Steroid Biochem. Mol. Biol. 127 (2011) 118–127, https://doi.org/10.1016/j.jsbmb.2010.10.004.

[3] J. Leadbitter, PVC and sustainability, Prog. Polym. Sci. 27 (2002) 2197–2226, https://doi.org/10.1016/S0079-6700(02)00038-2.

[4] J. Lopez-Cervantes, P. Paseiro-Losada, Determination of bisphenol A in, and its migration from, PVC stretch film used for food packaging, Food Addit. Contam. 20 (2003) 596–606, https://doi.org/10.1080/0265203031000109495.

[5] K. Inoue, S. Kondo, Y. Yoshie, K. Kato, Y. Yoshimura, M. Horie, H. Nakazawa, Migration of 4-nonylphenol from polyvinyl chloride food packaging films into food simulants and foods, Food Addit. Contam. 18 (2001) 157–164, https://doi.org/10.1080/02652030010018930.

[6] W.T. Piver, Organotin compounds: industrial applications and biological investigation, Environ. Health Perspect. 4 (1973) 61–79.

[7] S.W.C. Chung, A.H.T. Wu, Determination of butyltins, phenyltins and octyltins in foods with preservation of their moieties: a critical review on analytical methods, J. Chromatogr., A 1505 (2017) 18–34, https://doi.org/10.1016/j.chroma.2017.05.014.

[8] R. de C. Oliveira, R.E. Santelli, Occurrence and chemical speciation analysis of organotin compounds in the environment: a review, Talanta 82 (2010) 9–24, https://doi.org/10.1016/j.talanta.2010.04.046.

[9] J. Richter, I. Fettig, R. Philipp, N. Jakubowski, U. Panne, P. Fisicaro, E. Alasonati, Determination of tributyltin in whole water matrices under the European water framework directive, J. Chromatogr., A 1459 (2016) 112–119, https://doi.org/10.1016/j.chroma.2016.06.068.

[10] J. Szpunarlobinska, M. Ceulemans, W. Dirkx, C. Witte, R. Lobinski, F.C. Adams, Interferences IN ultratrace speciation OF organolead and organotin BY gas-chromatography with atomic spectrometric detection, Mikrochim. Acta 113 (1994) 287–298, https://doi.org/10.1007/BF01243619.

[11] P. Bermejo-Barrera, G. Gonzalez-Campos, M. Ferron-Novais, A. Bermejo-Barrera, Column preconcentration of organotin with tropolone-immobilized and their determination by electrothermal atomization absorption spectrometry, Talanta 46 (1998) 1479–1484, https://doi.org/10.1016/S0039-9140(98)00021-6.

[12] J. Sanz-Asensio, M.T. Martinez-Soria, M. Plaza-Medina, M.P. Clavijo, Simultaneous determination of organotin compounds by hydride generation-gas phase molecular absorption spectrometry, Talanta 54 (2001) 953–962, https://doi.org/10.1016/S0039-9140(01)00365-4.

[13] T. Hamasaki, Simultaneous determination of organotin compounds in textiles by gas chromatography-flame photometry following liquid/liquid partitioning with tert-butyl ethyl ether after reflux-extraction, Talanta 115 (2013) 374–380, https://doi.org/10.1016/j.talanta.2013.04.041.

[14] C. Coscolla, S. Navarro-Olivares, P. Marti, V. Yusa, Application of the experimental design of experiments (DoE) for the determination of organotin compounds in water samples using HS-SPME and GC-MS/MS, Talanta 119 (2014) 544–552,

https://doi.org/10.1016/j.talanta.2013.11.052.

[15] W. Hong, S. Weijian, W. Bin, Y. Keyao, J. Shan, L. Huiyuan, H. Guoshen, W. Yiqian, G. Ling, S. Jieming, Determination of organo-tin residues in edible vegetable oil by positive chemical ionizationgas chromatography-mass spectrometry, CHINESE J. Chromatogr. 37 (2019) 21–26, https://doi.org/10.3724/SP.J.1123.2018.09002.

[16] B. Qian, J. Zhao, Y. He, L. Peng, H. Ge, B. Han, A liquid chromatography detector based on continuous-flow chemical vapor generation coupled glow discharge atomic emission spectrometry: determination of organotin compounds in food samples, J. Chromatogr., A 1608 (2019), https://doi.org/10.1016/j. chroma.2019.460406.

[17] J. Sun, B. He, Y. Yin, L. Li, G. Jiang, Speciation of organotin compounds in environmental samples with semi-permanent coated capillaries by capillary electrophoresis coupled with inductively coupled plasma mass spectrometry, Anal. Methods 2 (2010) 2025–2031, https://doi.org/10.1039/c0ay00558d.

[18] G. Yang, J. Xua, L. Xu, G. Chen, F. Fu, Analysis of ultratrace triorganotin compounds in aquatic organisms by using capillary electrophoresis-inductively coupled plasma mass spectrometry, Talanta 80 (2010) 1913–1918, https://doi.org/10.1016/ j.talanta.2009.10.043.

[19] Y. Niu, F. Han, Q. Zhang, T. Xie, L. Lu, S. Li, H. Xia, Off/on fluorescent chemosensors for organotin halides based on binuclear ruthenium complexes, Angew. CHEMIE-INTERNATIONAL Ed. 52 (2013) 5599–5603, https://doi.org/10.1002/anie.201209549.

[20] S.-H. Li, F.-R. Chen, Y.-F. Zhou, J.-N. Wang, H. Zhang, J.-G. Xu, Enhanced fluorescence sensing of hydroxylated organotins by a boronic acid-linked Schiff base, Chem. Commun. (2009) 4179–4181, https://doi.org/10.1039/b906467b.

[21] Y.-F. Zhou, J.-N. Wang, S.-H. Li, J.-G. Xu, Near-infrared chromogenic sensing of organotin species by a cyclopalladated azo dye, Analyst 136 (2011) 282–284, https://doi.org/10.1039/c0an00538j.

[22] R. Fairman, Ben, Wahlen, Speciation analysis of organotin compounds by HPLC- ICP-MS, Spectroscopy, Spectrosc. Eur. 13 (2001) 16–23.

[23] J. Teran-Baamonde, S. Bouchet, E. Tessier, D. Amouroux, Development of a large volume injection method using a programmed temperature vaporization injector gas chromatography hyphenated to ICP-MS for the simultaneous determination of mercury, tin and lead species at ultra-trace levels in natural waters, J. Chromatogr., A 1547 (2018) 77–85, https://doi.org/10.1016/j.chroma.2018.02.056.

[24] K.E. Levine, D.J. Young, S.E. Afton, J.M. Harrington, A.S. Essader, F.X. Weber, R. A. Fernando, K. Thayer, E.E. Hatch, V.G. Robinson, S. Waidyanatha, Development, validation, and application of an ultra-performance liquid chromatography-sector field inductively coupled plasma mass spectrometry method for simultaneous determination of six organotin compounds in human serum, Talanta 140 (2015) 115–121, https://doi.org/10.1016/j.talanta.2015.03.022.

[25] T. Li, Y. She, M. Wang, G. Liu, H. Yu, J. Wang, S. Wang, F. Jin, M. Jin, H. Shao, Simultaneous determination of four organotins in food packaging by high- performance liquid chromatography-tandem mass spectrometry, Food Chem. 181 (2015) 347–353, https://doi.org/10.1016/j.foodchem.2015.02.115.

[26] P. Le Ru, Eric and Etchegoin, Principles of Surface Enhanced Raman Spectroscopy,

712 Elsevier, 2008.
713 [27] Z. Liu, L. Wang, W. Bian, M. Zhang, J. Zhan, Porous silver coating fiber for rapidly
714 screening organotin compounds by solid phase microextraction coupled with surface
715 enhanced Raman spectroscopy, RSC Adv. 7 (2017) 3117–3124, https://doi.
716 org/10.1039/c6ra25491h.
717 [28] K. V Arvanitoyannis, S. Ioannis, Kotsanopoulos, Migration phenomenon in food
718 packaging. Food–package interactions, mechanisms, types of migrants, testing and
719 relative legislation—a review, Food Bioprocess Technol. 7 (2014) 21–36.
720 [29] Y. Wan, Z. Guo, X. Jiang, K. Fang, X. Lu, Y. Zhang, N. Gu, Quasi-spherical silver
721 nanoparticles: aqueous synthesis and size control by the seed-mediated Lee-Meisel
722 method, J. Colloid Interface Sci. 394 (2013) 263–268, https://doi.org/10.1016/j.
723 jcis.2012.12.037.
724 [30] L. Mandrile, I. Cagnasso, L. Berta, A.M. Giovannozzi, M. Petrozziello, F. Pellegrino, A.
725 Asproudi, F. Durbiano, A.M. Rossi, Direct quantification of sulfur dioxide in wine by
726 Surface Enhanced Raman Spectroscopy, Food Chem. 326 (2020) 127009,
727 https://doi.org/10.1016/j.foodchem.2020.127009.
728 [31] A. Malengo, F. Pennecchi, A weighted total least-squares algorithm for any fitting model
729 with correlated variables, Metrologia 50 (2013) 654–662, https://doi.org/ 10.1088/0026-
730 1394/50/6/654.
731 [32] G. Wuebbeler, M. Krystek, C. Elster, Evaluation of measurement uncertainty and its
732 numerical calculation by a Monte Carlo method, Meas. Sci. Technol. 19 (2008),
733 https://doi.org/10.1088/0957-0233/19/8/084009.
734 [33] V.B.G.A. Shrivastava, Methods for the determination of limit of detection and limit of
735 quantitation of the analytical methods, Chronicles Young Sci. 2 (2011) 21,
736 https://doi.org/10.4103/2229-5186.79345.
737 [34] D. Pankin, I. Kolesnikov, A. Vasileva, A. Pilip, V. Zigel, A. Manshina, Raman
738 ingerprints for unambiguous identification of organotin compounds, Spectrochim. ACTA
739 PART A-MOLECULAR Biomol. Spectrosc. 204 (2018) 158–163, https://doi.
740 org/10.1016/j.saa.2018.06.044.
741 [35] G. Socrates, Infrared and Raman Characteristic Group Frequencies: Tables and Charts,
742 John Wiley & Sons, 2004.
743 [36] M.C. Tobin, Rotational isomerism and the vibrational spectra of dibutyltin dichloride, J.
744 Mol. Spectrosc. 5 (1961) 65–71.
745 [37] C.M. Cobley, S.E. Skrabalak, D.J. Campbell, Y. Xia, Shape-controlled synthesis of silver
746 nanoparticles for plasmonic and sensing applications, Plasmonics 4 (2009) 171–179,
747 https://doi.org/10.1007/s11468-009-9088-0.
748 [38] Y.N.Z. Riu Xiu He, Robert Liang, Peng Peng, Effect of the size of silver nanoparticles on
749 SERS signal enhancemen, J. Nanoparticle Res. 19 (2017) 267.
750 [39] S. Hong, X. Li, Optimal size of gold nanoparticles for surface-enhanced Raman
751 spectroscopy under different conditions, J. Nanomater. (2013), https://doi.org/
752 10.1155/2013/790323.